IEEE Access
Multidisciplinary | Rapid Review | Open Access Journal

Received July 28, 2018, accepted August 29, 2018, date of publication September 4, 2018, date of current version September 28, 2018.

Digital Object Identifier 10.1109/ACCESS.2018.2868497

Decoupling of Kinematic Parameter Identification for Articulated Arm Coordinate Measuring Machines

GUANBIN GAO, JUN ZHAO, AND JING NA, (Member, IEEE)
Faculty of Mechanical and Electrical Engineering, Kunming University of Science and Technology, Kunming 650500, China
Corresponding author: Guanbin Gao (gbgao@163.com)

This work was supported by the National Natural Science Foundation of China under Grant 51465027.

ABSTRACT Kinematic parameter identification is an effective method to improve the accuracy of articulated arm coordinate measuring machines (AACMMs). However, not all the parameters of AACMM can be identified accurately due to the influence of strong non-linear couplings. In this paper, we study the coupling relationship and then propose a decoupling method of AACMM parameters, which could retain the effectiveness of decoupling on parameter identification. The kinematic model of AACMM is established based on the DH method. The coupling relationship between kinematic parameters is obtained via the singular value decomposition. Then, the identification and compensation models are established. The least squares method is used to solve the identification model, and the kinematic parameters of the AACMM are identified. Simulation and experimental studies are carried out to verify the effectiveness of the proposed decoupling and identification methods. The results show that after decoupling, the accuracy of identification of the related coupling kinematic parameters is improved and the computational efficiency of identification is increased greatly.

INDEX TERMS Parameter identification, kinematics, decoupling, least squares method.

I. INTRODUCTION

Parameter identification has been widely used in many fields [1]–[3], such as robots and coordinate measuring machines. Coordinate measuring machines are mainly used in on-line detection, quality control and reverse engineering. With the strict requirement for the working environment and small measuring space, traditional coordinate measuring machines cannot be adopted in industrial field measurement. In recent years, some non-orthogonal coordinate measurement systems were developed to overcome the above mentioned problems of traditional coordinate measuring machines, e.g. laser tracking coordinate measuring systems, electronic latitude and longitude measurement systems, multi-vision sensor coordinate measurement systems, laser scanning systems and Articulated Arm Coordinate Measuring Machines (AACMM), etc.

Among different devices, AACMM is a series structure measurement system with the advantages of open measurement space, easy for operation and carrying, low environmental requirements and suitability of on-site measurement. However, as an open linkage type structure like industrial robots, the measurement accuracy of AACMM is relatively low due to the accumulation and amplification effect of the kinematic parameters' error of the serial joints. Parameter identification and compensation for improving the accuracy of AACMM have been a main topic in this field.

In this topic, Benciolini and Vitti [4] developed a mathematical model and algorithm of identification for the AACMM based on the operation characteristics. Acero *et al.* [5] studied different techniques to acquire data for verifying the parameter identification method of AACMM. Cheng *et al.* [6] proposed a non-redundant kinematic model and a simple identification method for AACMM by analyzing the structural parameters of the kinematic model. Daniel *et al.* [7] stated that one of the main principles of metrology was to reproduce the actual measurement process (the same instrument handling, environment, measurement parameters, etc.) during calibration to obtain the right information when calibrating the instrument. However, this principle is currently overlooked in the AACMM evaluation or calibration procedure. Luo *et al.* [8] tested the accuracy of AACMM based on the measured force,

whilst they did not consider the redundancy between the parameters for AACMM. For manipulators having a mix of both rotational and translational degrees of freedom, i.e., complex degree of freedom manipulators, the condition number of the Jacobian matrix may not be used due to the dimensional inconsistencies with its elements. In contrary, Pond and Carretero [9] further introduced alternative scheme to obtain a Jacobian matrix which may be used to determine the dexterity of parallel mechanisms regardless of the number and type of degrees of freedom of the mechanisms. A new method has been pioneered by Santolaria and Cajal [10], which uses a calibrated gauge object to develop a method for obtaining an inherent laser plane. This method does not require an additional optimization method after the previous sensor calibration. To solve the problem of working space, Piratelli-Filho *et al.* [11] analyzed the working space with the Monte Carlo method. To improve the accuracy of AACMM, Wang *et al.* [12] proposed a method of measuring pose optimization based on the clustering, which did not consider the influence of redundancy on accuracy. To compensate for the insufficient measurement model, Zheng *et al.* [13] constructed a number of DH measurement models and solved the structural parameters via the Levenberg-Marquardt calibration algorithm. Zheng *et al.* [14] analyzed the circular grating eccentricity of AACMM and obtained the model parameters of the circular grating eccentricity error of 6 joints via circular grating eccentricity error. Then, the calibration operation of the measurement model was completed by using homemade standard components.

In viewing available methods, it is found that the quality of parameters identification of AACMM depends on the scope of the effective solution or the promotion capability [15], [16]. However, at present, few studies focus on this problem. In this paper, the validity of kinematic parameter identification of AACMM is simulated and experimentally studied. The main contribution of this paper can be summarized as follows:

1) The coupling relationship of kinematic parameters of AACMM is analyzed by singular value decomposition, which shows that not all the parameters of AACMM can be identified accurately due to the influence of strong non-linear couplings.
2) A new decoupling method for parameter identification of AACMM is proposed, which can decrease the computation and increase the accuracy of identification.
3) Parameter identification and compensation model of AACMM are established, which are then used to improve the accuracy of AACMM.

II. THE COUPLING RELATIONSHIP OF KINEMATIC PARAMETERS OF AACMM

A. KINEMATIC MODELING

The essence of kinematic modeling is to study the relationship between the joint variables and the position coordinates of the probe, which is the basis of our research work. Nenchev [17] proposed a generic model in 1956. The model is with a 4×4 coordinate transformation matrix to describe the relationship between adjacent links, which derived the transformation matrix of the "end effector coordinate system" relative to the "base coordinate system". There are many advantages for DH model. Firstly, it is easy to be understood and programed. Secondly, it can be used widely in the kinematics analysis of the robot, and also for kinematics analysis of AACMM.

The DH model strictly defines the coordinate system between the links. Firstly, a base coordinate system ($\{x_0, y_0, z_0\}$) is set based on the AACMM. Then, six coordinate systems are established on the joints 1 to 6 ($\{x_i, y_i, z_i\}$). It is worth noting that the base coordinate system maintains are fixed and the remaining six coordinate systems follow the joint movement in the working of AACMM. The basic principles are given as follows:

1) One determines the z axis of each coordinate system and the z_i axis goes along the axial direction of the joint $i+1$.
2) One determines the origin O of each coordinate system and selects the origin O_i on the common normal of z_{i-1} axis and z_i axis.
3) One determines the x axis of the coordinate system; x_i axis goes along the common normal between z_i axis and z_{i-1} axis and points to the leaving direction of z_{i-1}.
4) One determines the y axis of the coordinate system and sets $y_i = x_i + z_i$.

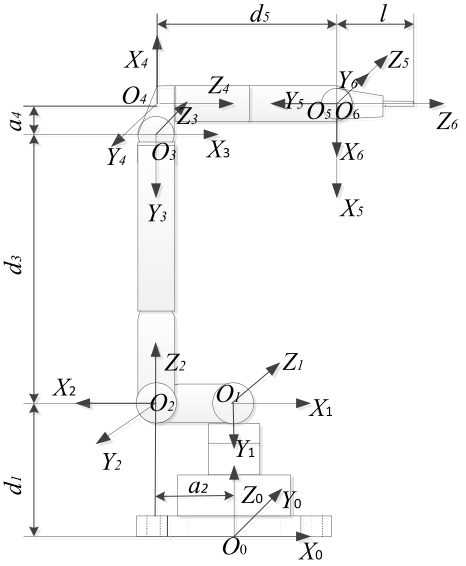

FIGURE 1. The coordinate systems of the AACMM.

According to the above steps, the establishment of a measuring machine coordinate system can be shown in Figure.1. Then, we can obtain the kinematic parameters of AACMM. That is, the length of linkages, the length of joints, the twist angle of linkages and the angle of joints. There are six parameters contained in each group. The kinematic parameters of AACMM are determined as follows:

1) Link length, a_{i-1} is the distance from z_{i-1} to z_i along x_{i-1}.

2) Twist angle, α_{i-1} is the angle between z_{i-1} to z_i along x_{i-1}.
3) Offset length, d_i is the distance from x_{i-1} to x_i along x_{i-1}.
4) Joint angle, θ_i is the angle between x_{i-1} to x_i along z_i.

Among the four groups of parameters, only θ_i are variable, and the remaining three groups of parameters are with fixed values. According to the above definition, the kinematic parameters of AACMM can be obtained by measurement, and some related parameters can be shown in Table.1. The joint rotation angle θ_i of the AACMM is in the range of: $\theta_1 \in [-180, 180]$, $\theta_2 \in [-180, 180]$, $\theta_3 \in [-180, 180]$, $\theta_4 \in [-180, 180]$, $\theta_5 \in [-180, 180]$, $\theta_6 \in [-180, 180]$.

TABLE 1. The nominal kinematic parameters of the AACMM.

Linkage No. i	a_i[mm]	d_i[mm]	$\Delta\theta_i$[°]	α_i[°]	l[mm]
1	0	376	0	-90	98
2	62	0	0	-90	
3	0	751	0	-90	
4	62	0	0	-90	
5	0	500	0	-90	
6	0	15	0	90	

The transformation matrix $T_{i-1,i}$ of the coordinate system from $\{x_{i-1}, y_{i-1}, z_{i-1}\}$ to $\{x_i, y_i, z_i\}$ can be achieved by rotation and translation. A coordinate system of the linkage can be established via the DH method. So one can get the transformation matrix (1) [18]:

$$T_{i-1,i} = Rot(z_{i-1}, \theta_i)Trans(0, 0, d_i)Trans(a_i, 0, 0)Rot(x_i, \alpha_i) = \begin{bmatrix} \cos\theta_i & -\sin\theta_i\cos\alpha_i & \sin\theta_i\sin\alpha_i & a_i\cos\theta_i \\ \sin\theta_i & \cos\theta_i\cos\alpha_i & -\cos\theta_i\sin\alpha_i & a_i\sin\theta_i \\ 0 & \sin\alpha_i & \cos\alpha_i & d_i \\ 0 & 0 & 0 & 1 \end{bmatrix} \tag{1}$$

The transformation matrix between $\{x_6, y_6, z_6\}$ and $\{x_0, y_0, z_0\}$ can be obtained via pre-multiplying the transformation matrix between a frame and the previous one, which is shown in (2).

$$T_{0,6} = T_{0,1} \cdot T_{1,2} \cdot T_{2,3} \cdot T_{3,4} \cdot T_{4,5} \cdot T_{5,6} \tag{2}$$

If the coordinates of the probe sphere center in $\{x_6, y_6, z_6\}$ is $(0, 0, l)$, its coordinates in the base frame of $\{x_0, y_0, z_0\}$ can be calculated via (3)

$$P = T_{0,6} \times [0, 0, l, 1]^{\mathrm{T}} \tag{3}$$

B. COUPLING RELATIONSHIP OF THE PARAMETERS

In some cases, the Jacobian matrix J is a singular matrix for linearly related parameters existed in the model. Therefore, the solutions of least squares are not the desired values. To acquire desired values, it is necessary to carry out the decomposition of singular values for the Jacobian matrix and find the linear correlation quantity in terms of the parallel transformation of the orthogonal array after decomposition. Then the parameters to be identified are determined [19].

$$[J^{\mathrm{T}} \cdot J] \times \Delta X = J^{\mathrm{T}} \cdot \Delta P \tag{4}$$

Considering $H = [J^T \cdot J]$, one can obtain (5) via singular value decomposition for H:

$$H = U \cdot \begin{bmatrix} \Sigma & 0 \\ 0 & 0 \end{bmatrix} \cdot V^{\mathrm{T}} \tag{5}$$

where U and V are orthogonal matrices, $\sum = diag(\sigma_1, \sigma_2 \cdots, \sigma_r)(r \leq 25)$, r is the rank of the matrix H, that is, r is the rank of the Jacobian matrix J. One can further know that the number of linearly related parameters is 25-r in the 25 geometric parameters. We substitute formula (5) into (4) and can get:

$$V^{\mathrm{T}} \cdot \Delta X = \begin{bmatrix} \Sigma^1 & 0 \\ 0 & 0 \end{bmatrix} \cdot U^{-1} \cdot J^{-\mathrm{T}} \cdot \Delta P \tag{6}$$

where $V^{\mathrm{T}} = U^{-1}$, V is a rotation matrix. In (6), $V^{\mathrm{T}} \cdot \Delta X$ is equivalent to the rotation of ΔX, and the linear correlation parameters are in the same zero plane. One can acquire linearly related parameters via an elementary row transformation for the last 25-r line of V^{T}. The linearly related parameters can be written as:

$$\Delta a_6 = l\Delta\theta_6 \tag{7}$$

$$\Delta d_6 = -l\Delta\alpha_6 \tag{8}$$

According to the above equations, the kinematic parameters that need to be identified can be determined, and the other kinematic parameters can be removed from identification model. Then, the column of the corresponding Jacobian matrix is removed. The equation of coordinate error of the probe space can be calculated according to (9).

$$\Delta P = J_r \cdot \Delta X_r \tag{9}$$

The equation of kinematic parameter error can be calculated by (9) as:

$$\Delta X_r = (J_r^{\mathrm{T}} \cdot J_r)^{-1} J_r^{\mathrm{T}} \Delta P \tag{10}$$

where J_r is a matrix of $(3 \times n) \times r$, ΔX_r is a matrix of $r \times 1$ and ΔP is a matrix of $(3 \times n) \times 1$. One can obtain the kinematic parameter error via (10).

III. IDENTIFICATION MODELING

The least square method is a basic method which can deal with various observational data to measure the mean difference.

The least square method [20] can be formulated as follows: there are given data $(x_i, y_i)(i = 0, 1, 2, \cdots, n)$, $p(x) \in \phi$, which can be solved in the function class to make the square of the error and $v_i = p(x_i) - y_i(i = 0, 1, 2, \cdots, n)$. Then, the least square formulation satisfies:

$$\sum_{i=1}^{m} v_i^2 = \sum_{i=1}^{m} (y_i - f(x_i; b))^2 = \min.$$

The least square method is easy to program and understand. Therefore, it has been widely utilized in kinematic parameter identification. To solve the equation group $\Delta P = J \cdot \Delta X$ in Matlab software, the solution given in (11) can be used.

$$\Delta X = \left(J^T \cdot J\right)^{-1} \cdot J^{\mathrm{T}} \cdot \Delta P \tag{11}$$

In this paper, a program is compiled based on the least square method by using Matlab, which can be used to solve the kinematic parameter errors for AACMM. The process of identification algorithm can be displayed as Figure. 2.

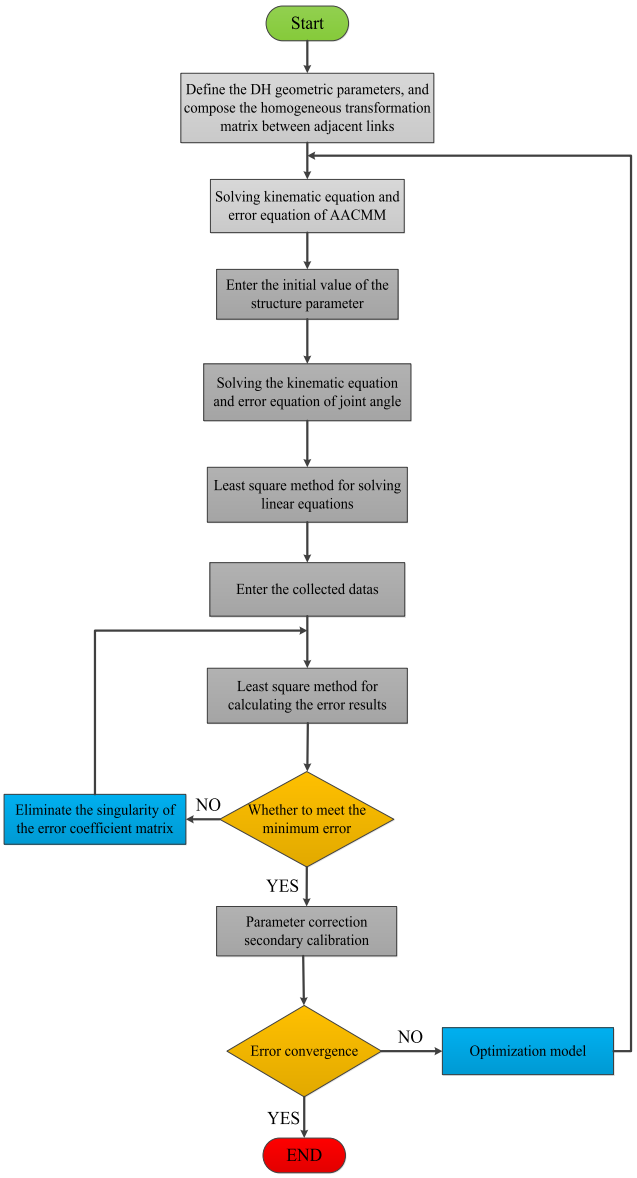

FIGURE 2. The flow chart of the identification algorithm.

IV. SIMULATION

A. THE ERROR OF THE AACMM BEFORE CALIBRATION

According to the previous analysis, parameters to be identified of AACMM with DH model are 25 and the number of collection points should be no less than 9. In the identification of simulation, one assumes that error values of d_i and a_i are 0.5mm, the error values of α_i and θ_i are 0.1° C, as shown in Table.2. One acquires 50 groups of data for kinematic parameter identification, then the angles of joints and coordinate values of the probe are obtained by kinematic modeling and calculated with the kinematic parameters of Table.2, respectively. The kinematic parameters in Table.2 and the probe coordinate values calculated from the kinematic parameters of Table.2 are considered as the accurate values.

TABLE 2. The error settings of DH parameters of the AACMM.

Linkage No. i	a_i+Δa_i[mm]	d_{i+}+Δd_i[mm]	$\Delta\theta_i$+$\Delta\theta_i$[°]	α_i+$\Delta\alpha_i$[°]
1	0+0.5	376+0.5	θ_1+0.1	-90-0.1
2	62+0.5	0+0.5	θ_2+0.1	-90-0.1
3	0+0.5	751+0.5	θ_3+0.1	-90-0.1
4	62+0.5	0+0.5	θ_4+0.1	-90-0.1
5	0+0.5	500+0.5	θ_5+0.1	-90-0.1
6	0+0.5	15+0.5	θ_6+0.1	90+0.1
		l+Δl=(98+0.5)mm		

B. THE SIMULATION OF IDENTIFICATION BEFORE DECOUPING

One considers the values are the nominal values in Table.2. Then we can obtain error values for probe coordinate via the calculated coordinate value via Table.2 and obtain the error values for kinematic parameters by solving 150 equations based on the obtained error values of probe coordinate. Then one acquires the kinematic parameter error values of AACMM with DH method to compensate the kinematic parameters. The kinematic parameters after identification are shown as Table.3.

TABLE 3. The identification results before decoupling.

Linkage No. i	a_i+Δa_i[mm]	d_{i+}+Δd_i[mm]	$\Delta\theta_i$+$\Delta\theta_i$[°]	α_i+$\Delta\alpha_i$[°]
1	0+0.493	376+0.496	θ_1+0.100	-90-0.100
2	62+0.501	0+0.498	θ_2+0.100	-90-0.100
3	0+0.500	751+0.506	θ_3+0.101	-90-0.100
4	62+0.488	0+0.485	θ_4+0.098	-90-0.100
5	0+0.502	500+0.496	θ_5+0.104	-90-0.028
6	0+0.000	15+0.000	θ_6+0.390	89.809
		l+Δl=(98+0.003)mm		

One can find from Table.2 and Table.3 that the DH kinematic parameters are more accurate except a_6, d_6, θ_6 and α_6.

To verify the effectiveness of the identification results, kinematic parameters given in Table.3 are substituted into the kinematic model. Then one collects 100 groups reference values to verify the validity of the identification results via the calculated errors between the reference values and

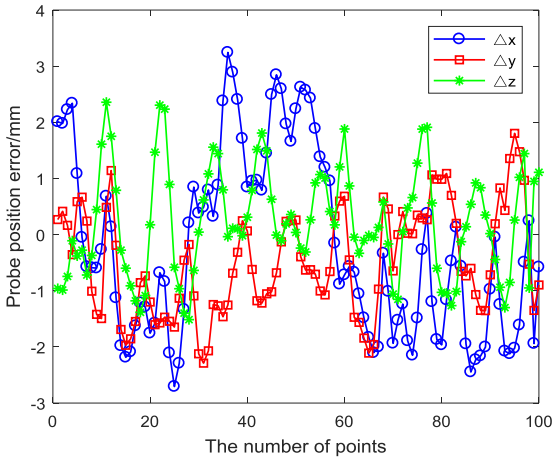

FIGURE 3. The error before identification without decoupling.

TABLE 4. The position error before identification without decoupling in simulation.

Probe coordinates	Maximum error (mm)	Standard deviation (mm)	The average of the maximum absolute value (mm)
x	3.244	1.609	1.409
y	-2.289	0.956	0.902
z	2.358	0.955	0.781

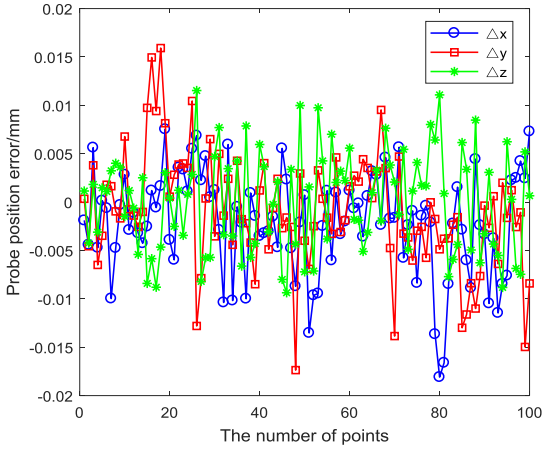

FIGURE 4. The error after identification without decoupling.

coordinates. The errors of probe before identification are shown in Figure.3 and Table.4. It is found that the maximum error is 3.244mm in three directions of x, y, z, the maximum standard deviation is 1.609mm, and the average value of the maximum absolute value is 1.409mm. The error of the probe after identification is shown in Figure.4 and Table.5, where the maximum error is -0.018mm in three directions x, y, z, the maximum standard deviation is 0.006mm, and the average value of the maximum absolute value is 0.004mm, respectively. The simulation in case of decoupling is continued to clarify the influence of redundancy on the identification of AACMM parameters.

TABLE 5. The position error after identification without decoupling in simulation.

Probe coordinates	Maximum error (mm)	Standard deviation (mm)	The average of the maximum absolute value (mm)
x	-0.018	0.005	0.004
y	-0.017	0.006	0.004
z	0.012	0.005	0.004

C. THE SIMULATION OF IDENTIFICATION AFTER DECOUPLING

1) THE ERROR WITHOUT IDENTIFICATION OF REDUNDANCY PARAMETERS

From equation (7) and (8), one knows that a_6 is linearly related to θ_6, d_6, which is linearly related to α_6. The rank of the Jacobian matrix is 23, which indicates that the Jacobian matrix is not a column full rank matrix and thus all DH kinematic parameters cannot be accurately identified. To obtain accurate results of identification, one removes the θ_6 and α_6 in the model of identification, and θ_6 and α_6 are not setting error values. The corresponding identification results can be displayed in Table.6.

TABLE 6. The identification results after decoupling without error settings of θ_6 and α_6.

Linkage No. i	a_i+Δa_i[mm]	d_{i+}+Δd_i[mm]	$\Delta\theta_i$+$\Delta\theta_i$[°]	α_i+$\Delta\alpha_i$[°]
1	0+0.500	376+0.503	θ_1+0.100	-90-0.099
2	62+0.501	0+0.504	θ_2+0.100	-90-0.100
3	0+0.497	751+0.500	θ_3+0.099	-90-0.100
4	62+0.492	0+0.476	θ_4+0.099	-90-0.097
5	0+0.500	500+0.498	θ_5+0.094	-90-0.090
6	0+0.499	15+0.516	θ_6+	90+
		l+Δl=(98+0.500)mm		

One can find that the DH kinematic parameters are more accurate by comparing Table.2 and Table.6.

The kinematic parameters given in Table.6 are substituted into the kinematic model. Then one collects 100 groups reference values to verify the validity of the identification results via the calculated errors between the reference values and the coordinates. The position errors before identification are shown in Figure.5 and Table.7. The maximum error is 3.240mm in three directions x, y, z. The maximum standard deviation is 1.775mm. The average value of the maximum absolute value is 1.654mm. The error of the probe after identification is shown in Figure.6 and Table.8. The maximum error is -0.024mm in three directions x, y, z, the maximum standard deviation is 0.006mm, and the average value of the maximum absolute value is 0.004mm.

We will proceed to the following simulation to further studying the differences, when the identification parameters have errors or not.

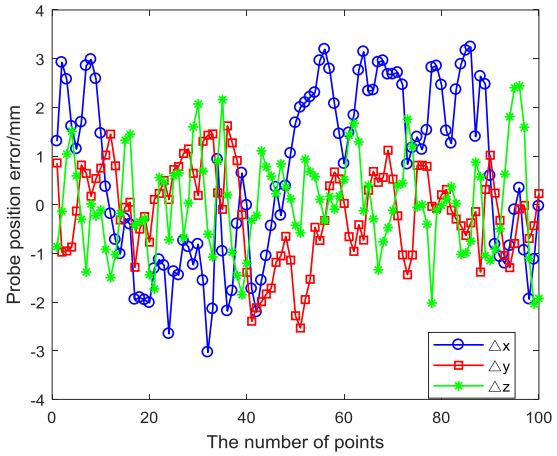

FIGURE 5. The position error before identification with decoupling.

TABLE 7. The position error before identification without decoupling in simulation.

Probe coordinates	Maximum error (mm)	Standard deviation (mm)	The average of the maximum absolute value (mm)
x	3.240	1.775	1.654
y	-2.533	0.954	0.771
z	2.441	1.020	0.809

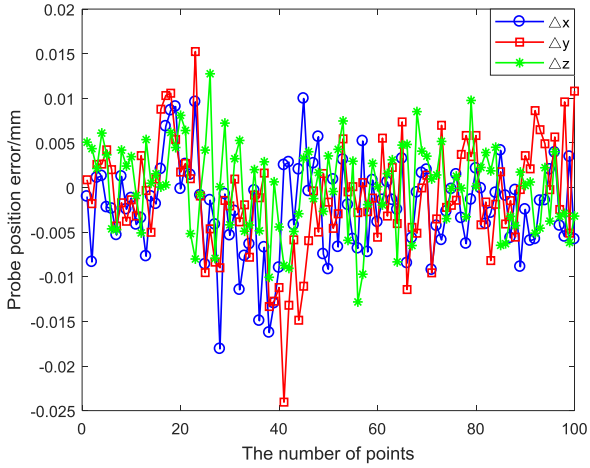

FIGURE 6. The position error after identification with decoupling.

TABLE 8. The position error after identification without decoupling in simulation.

Probe coordinates	Maximum error (mm)	Standard deviation (mm)	The average of the maximum absolute value (mm)
x	-0.018	0.005	0.004
y	-0.024	0.006	0.004
z	0.013	0.005	0.004

2) THE ERROR WITH IDENTIFICATION OF REDUNDANCY PARAMETERS

In the following simulation, θ_6 and α_6 are removed in the model of identification. At the same time, θ_6 and α_6 are set with errors. The related parameters can be shown in Table.9.

TABLE 9. The identification results after decoupling without error settings of θ_6 and α_6.

Linkage No. i	a_i+Δa_i[mm]	d_{i+}+Δd_i[mm]	$\Delta\theta_i$+$\Delta\theta_i$[°]	α_i+$\Delta\alpha_i$[°]
1	0+0.495	376+0.496	θ_1+0.100	-90-0.100
2	62+0.501	0+0.498	θ_2+0.100	-90-0.100
3	0+0.500	751+0.506	θ_3+0.101	-90-0.100
4	62+0.488	0+0.485	θ_4+0.098	-90-0.099
5	0+0.502	500+0.496	θ_5+0.104	-90-0.100
6	0+0.667	15+0.327	θ_6+	90+
		l+Δl=(98+0.000)mm		

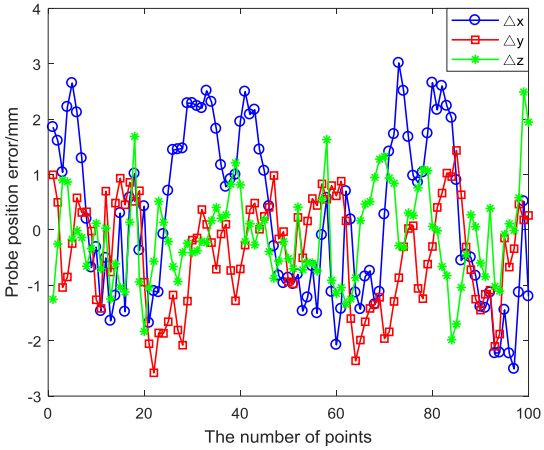

FIGURE 7. The position error before identification with decoupling.

TABLE 10. The position error before identification with decoupling in simulation.

Probe coordinates	Maximum error (mm)	Standard deviation (mm)	The average of the maximum absolute value (mm)
x	3.015	1.484	1.331
y	-2.580	0.961	0.838
z	2.490	0.830	0.666

Similarly, the kinematic parameters in Table.9 are substituted into the kinematic model. Then one collects 100 groups of reference values to verify the validity of the identification results via the calculated errors between the reference values and the coordinates. The errors of the probe before identification are shown in Figure.7 and Table.10. The maximum error is 3.015mm in three directions x, y, z. The maximum standard deviation is 1.484mm, the average value of maximum absolute value is 1.331mm and the errors of probe after identification are shown in Figure.8 and Table.11. The maximum error is -0.020mm in three directions x, y, z. The maximum standard deviation is 0.007mm.

D. COMPARISION AND ANALYSIS

One can find that the identification results given in Tables of 6 and 9 are more accurate when comparing the kinematic parameters given in Tables of 3, 6 and 9.

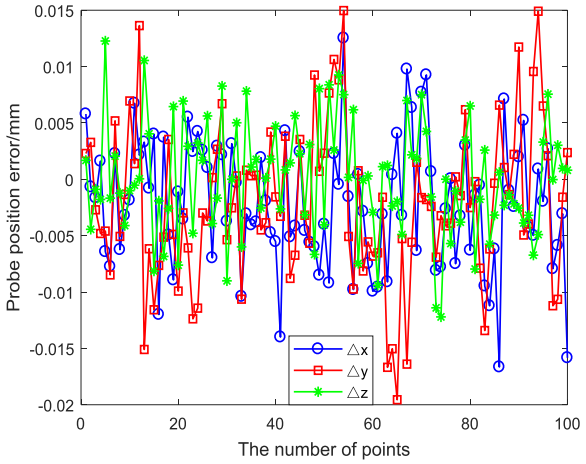

FIGURE 8. The position error after identification with decoupling.

TABLE 11. The position error after identification with decoupling in simulation.

Probe coordinates	Maximum error (mm)	Standard deviation (mm)	The average of the maximum absolute value (mm)
x	-0.017	0.006	0.005
y	-0.020	0.007	0.006
z	0.012	0.005	0.004

From equation (7) and (8), we know that a_6 is linearly related to θ_6 and d_6 is linearly related to α_6, which indicates that the results of accurate identification can be obtained via DH kinematic parameters in the presence of decoupling.

By comparing Tables of 5, 8 and 11, one can find that the errors are smaller after identification as shown in Table.8 and Table.11, which also indicates that the position accuracy of the probe is higher in the presence of decoupling.

V. EXPERIMENTS

A. THE ERROR OF AACMM BEFORE CALIBRATION

In this part, we conduct experiments to valid the previously introduced methods. In this case, data acquisition software is used to collect 50 groups of data and reference values for kinematic parameter identification experiments based on simulation results given in the Section IV. The experimental equipment is shown in Figure.9. The test environment temperature is $20 \pm 2^\circ$ C and environment humidity is about 30%. One collects 50 groups of data for kinematic parameter identification to study the effect of data on kinematic parameters identification under this environment conditions. The nominal kinematic parameters are shown in Table.1.

B. THE IDENTIFICATION BEFORE DECOUPLING

The kinematic parameters in Table.12 are substituted into the kinematic model. Then one collects 100 groups of reference values to verify the validity of the identification results via the calculated errors between the reference values and the coordinates. The errors of the probe before identification are shown

FIGURE 9. The articulated arm coordinate measuring machine used in experiments.

TABLE 12. The identification results before decoupling.

Linkage No. i	a_i[mm]	d_i[mm]	$\Delta\theta_i$[°]	α_i[°]
1	0.016	376.554	0.078	-89.990
2	62.133	-0.045	-0.021	-90.018
3	0.068	750.562	0.006	-90.002
4	61.742	0.071	-0.069	-89.997
5	-0.061	500.310	0.092	-90.012
6	0	15.000	0.003	89.985
		l=97.941mm		

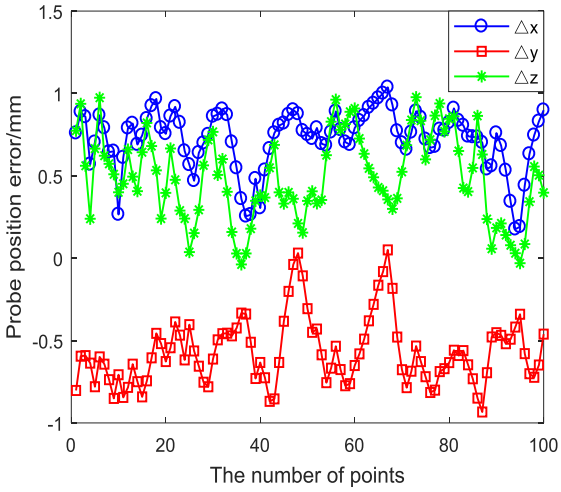

FIGURE 10. The position error before identification without decoupling.

in Figure.10 and Table.13. The maximum error is 1.037mm in three directions x, y, z. The maximum standard deviation is 0.262mm, and the average value of maximum absolute value is 0.724mm. The errors of probe after identification are shown in Figure.11 and Table.14. The maximum error x, y, z is -0.114mm in three directions. The maximum standard deviation is 0.030mm. The average value of the maximum

TABLE 13. The position error before identification without decoupling in test.

Probe coordinates	Maximum error (mm)	Standard deviation (mm)	Time cost (s)	RAM cost (%)
x	1.037	0.180		
y	-0.934	0.204	1020	16.6
z	0.977	0.262		

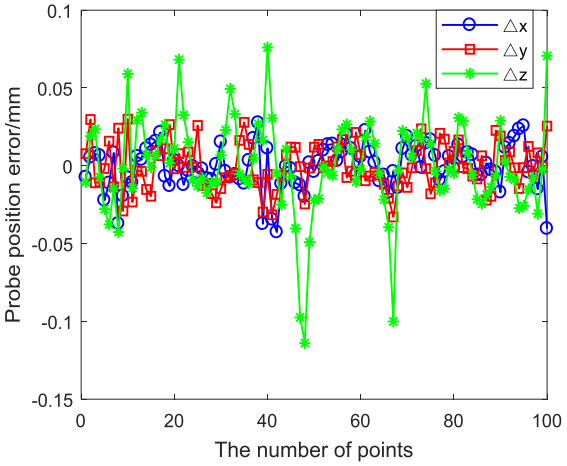

FIGURE 11. The position error after identification without decoupling.

TABLE 14. The position error after identification without decoupling in test.

Probe coordinates	Maximum error (mm)	Standard deviation (mm)	Time cost (s)	RAM cost (%)
x	-0.043	0.014		
y	-0.033	0.015	1020	16.6
z	-0.114	0.030		

absolute value is 0.022mm. To clear the effect of redundancy on AACMM parameter identification, one will continue the experiment with decoupling.

C. THE IDENTIFICATION AFTER DECOUPLING

From the fourth part, in the case of decoupling, the errors of identification parameters do not affect the identification results. Therefore, in the case of decoupling, the identification experiment only discusses that there is no error for identification parameters.

One knows that a_6 is linearly related to θ_6 and d_6 is linearly related to α_6 from part B of Section II. The model of identification is removed θ_6, α_6 to obtain accurate results of identification in the following experiment. 50 groups of data for identification results can be shown in Table.15.

Similarly, the kinematic parameters given in Table.15 are substituted into the kinematic model. Then, we collect 100 groups of reference values to verify the validity of the identification results via the calculated errors between the

TABLE 15. The identification results after decoupling without identification of θ_6 and α_6.

Linkage No. i	a_i[mm]	d_i[mm]	$\Delta\theta_i$[°]	α_i[°]
1	0.160	376.490	0.037	-90.007
2	62.205	-0.010	-0.021	-89.980
3	0.044	750.445	-0.015	-90.001
4	61.871	-0.013	-0.057	-89.987
5	-0.073	500.276	0.099	-90.001
6	0.073	15.024	0	90
		l=97.974mm		

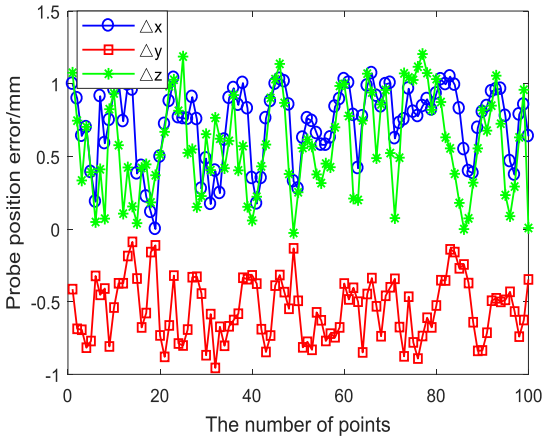

FIGURE 12. The position error before identification with decoupling.

TABLE 16. The position error before identification in decoupling test.

Probe coordinates	Maximum error (mm)	Standard deviation (mm)	Time cost (s)	RAM cost (%)
x	1.072	0.260		
y	-0.956	0.212	420	15.1
z	1.204	0.335		

reference values and the coordinates. The errors of the probe before identification are shown in Figure.12 and Table.16.

The maximum error is 1.204mm in three directions x, y, z. The maximum standard deviation is 0.335mm. The average value of the maximum absolute value is 0.824mm. The errors of the probe after identification are shown in Figure.13, Table.17. The maximum error x, y, z is -0.103mm in three directions. The maximum standard deviation is 0.029mm. The average value of the maximum absolute value is 0.021mm.

D. COMPARISON AND ANALYSIS

One can find from above results that the errors are reduced after parameter identification before decoupling when comparing Table.13, Table.14 and Figure.10, Figure.11, and the errors after identification are also reduced and the proposed method can greatly decrease the computational efficiency of identification in the case of decoupling by comparing Table.16, Table.17 and Figure.12, Figure.13.

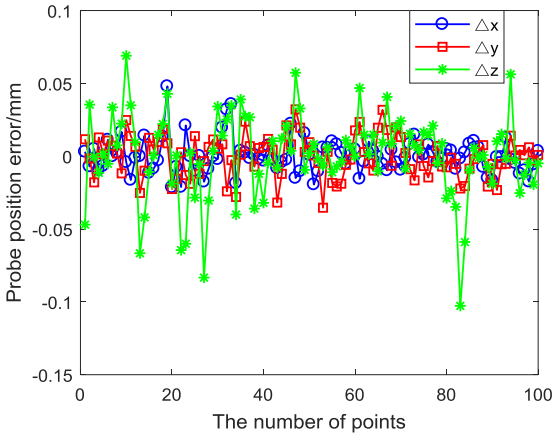

FIGURE 13. The position error after identification with decoupling.

TABLE 17. The position error after identification in decoupling test.

Probe coordinates	Maximum error (mm)	Standard deviation (mm)	Time cost (s)	RAM cost (%)
x	0.048	0.012		
y	-0.035	0.014	420	15.1
z	-0.103	0.029		

We also find that the errors after parameter identification are minimized in the presence of decoupling by comparing Table.14, Table.17 and Figure.11, Figure.13. In this situation, the maximum error is reduced by about 10%, the standard deviation is reduced by about 4% and the average of the absolute values is reduced by about 5%. Therefore, AACMM parameter identification can remove θ_6 and α_6 to increase the accuracy and speed of the identification.

VI. CONCLUSION

The coupling relationship between kinematic parameters of AACMM influences the identification and calibration performance greatly. This problem is studied through mathematical analysis, simulations and experiments in this paper. Jacobian matrix and singular value decomposition are used to determine the coupling relationship of the AACMM parameters. Then, a parameter identification model is established based on the kinematic model and the least squares method. Simulations were conducted to test the effectiveness of decoupling. The results showed that the identification model is effective regardless of decoupling, whist the linearly related kinematic parameters cannot be identified accurately without decoupling. After carrying out the decoupling, the accuracy of identification is improved and the identification calculation is decreased as well. Experiments with an AACMM were carried out to test the suggested decoupling and identification methods, which also showed that the accuracy of the AACMM is improved after decoupling.

REFERENCES

[1] N. Tan, X. Gu, and H. Ren, "Simultaneous robot-world, sensor-tip, and kinematics calibration of an underactuated robotic hand with soft fingers open access," *IEEE Access*, vol. 6, pp. 22705–22715, 2017.
[2] L. Liu, L. Shan, Y. Dai, C. Liu, and Z. Qi, "A modified quantum bacterial foraging algorithm for parameters identification of fractional-order system," *IEEE Access*, vol. 6, pp. 6610–6619, 2018.
[3] K. Ostrowska, A. Gąska, R. Kupiec, J. Sładek, and K. Gromczak, "Verification of articulated arm coordinate measuring machines accuracy using lasertracer system as standard of length," *Mapan*, vol. 31, no. 4, pp. 241–256, Dec. 2016.
[4] B. Benciolini and A. Vitti, "A new quaternion based kinematic model for the operation and the identification of an articulated arm coordinate measuring machine inspired by the geodetic methodology," *Mechanism Mach. Theory*, vol. 112, pp. 192–204, Jun. 2017.
[5] R. Acero, A. Brau, J. Santolaria, and M. Pueo, "Evaluation of a metrology platform for an articulated arm coordinate measuring machine verification under the ASME B89.4.22-2004 and VDI 2617_9-2009 standards," *J. Manuf. Syst.*, vol. 42, pp. 57–68, Jan. 2017.
[6] W. Cheng, Y. Fei, L. Yu, and R. Yang, "Probe parameters calibration for articulated arm coordinate measuring machine," in *Proc. SPIE*, Hubei, China, 2009, pp. 75445K–75451K.
[7] G. M. Daniel, B. Joaquín, C. Eduardo, and M. P. Susana, "Influence of human factor in the AACMM performance: A new evaluation methodology," *Int. J. Precis. Eng. Manuf.*, vol. 15, no. 7, pp. 1283–1291, 2014.
[8] Z. Luo *et al.*, "Error analysis and compensation of the measuring force of the articulated arm coordinate measuring machine," *Yi Qi Yi Biao Xue Bao/Chin. J. Sci. Instrum.*, vol. 38, no. 5, pp. 1159–1167, 2017.
[9] G. Pond and J. A. Carretero, "Formulating Jacobian matrices for the dexterity analysis of parallel manipulators," *Mechanism Mach. Theory*, vol. 41, no. 12, pp. 1505–1519, 2006.
[10] J. Santolaria, J.-J. Aguilar, D. Guillomía, and C. Cajal, "A crenellated-target-based calibration method for laser triangulation sensors integration in articulated measurement arms," *Robot. Comput.-Integr. Manuf.*, vol. 27, no. 2, pp. 282–291, 2011.
[11] A. Piratelli-Filho, F. H. T. Fernandes, and R. V. Arencibia, "Application of virtual spheres plate for AACMMs evaluation," *Precis. Eng.*, vol. 36, no. 2, pp. 349–355, 2012.
[12] J. Wang, Y. Guo, L. Zhu, and Z. Pan, "Measuring posture optimization for articulated arm coordinate measuring machine based on cluster," *Modern Manuf. Eng.*, vol. 2017, pp. 141–144, Mar. 2017.
[13] D. Zheng, Z. Xiao, and X. Xia, "Multiple measurement models of articulated arm coordinate measuring machines," *Chin. J. Mech. Eng.*, vol. 28, no. 5, pp. 994–998, 2015.
[14] D. Zheng, S. Yin, Z. Luo, J. Zhang, and T. Zhou, "Measurement accuracy of articulated arm CMMs with circular grating eccentricity errors," *Meas. Sci. Technol.*, vol. 27, no. 11, p. 115011, 2016.
[15] C. Hu, X. Liu, W. Yang, W. Lu, N. Yu, and S. Chang, "Improved zero-order fringe positioning algorithms in white light interference based atomic force microscopy," *Opt. Lasers Eng.*, vol. 100, pp. 71–76, Jan. 2018.
[16] G. Gao, H. Zhang, H. San, X. Wu, and W. Wang, "Modeling and error compensation of robotic articulated arm coordinate measuring machines using BP neural network," *Complexity*, vol. 2017, pp. 264–271, Oct. 2017.
[17] D. N. Nenchev and Z. M. Sotirov, "Dynamic task-priority allocation for kinematically redundant robotic mechanisms," in *Proc. IEEE Int. Conf. Robot. Automat.*, San Diego, CA, USA, Sep. 1994, pp. 518–524.
[18] G. Gao, H. Zhang, X. Wu, and Y. Guo, "Structural parameter identification of articulated arm coordinate measuring machines," *Math. Problems Eng.*, vol. 2016, pp. 1–10, Sep. 2016.
[19] G. Gao, J. Na, X. Wu, and Y. Guo, "A self-calibration method for articulated arm coordinate measuring machines," *Trans. Can. Soc. Mech. Eng.*, vol. 40, no. 4, pp. 645–655, 2016.
[20] W. Yang, X. Liu, W. Lu, C. Hu, and X. Guo, "Towards a traceable probe calibration method for white light interference based AFM," *Precis. Eng.*, vol. 51, pp. 40–47, Jan. 2017.

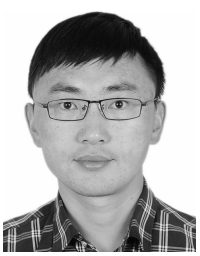

GUANBIN GAO received the B.Sc. and M.Sc. degrees in mechanical engineering and automation from Northeastern University, Shenyang, China, in 2001 and 2004, respectively, and the Ph.D. degree in mechanical manufacturing and automation from Zhejiang University, Hangzhou, China, in 2010. He is currently an Associate Professor at the Kunming University of Science and Technology.

His research mainly focuses on precision measuring and control, kinematics of industrial robots, and neural networks.

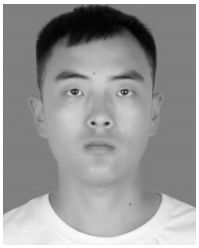

JUN ZHAO received the B.Sc. degree in mechanical design, manufacturing and automation from the Qingdao University of Science and Technology, Qingdao, China, in 2016. He is currently pursuing the Ph.D. degree at the Kunming University of Science and Technology, Kunming, China.

His current research interests include robust control optimal control and kinematics parameter identification of industrial robots.

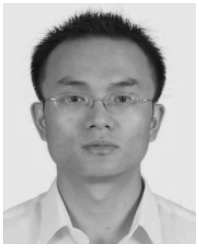

JING NA (M'15) received the B.Sc. and Ph.D. degrees from the School of Automation, Beijing Institute of Technology, Beijing, China, in 2004 and 2010, respectively. From 2011 to 2013, he was a Monaco/ITER Post-Doctoral Fellow at the ITER Organization, France. From 2015 to 2017, he was a Marie Curie Intra-European Fellow with the Department of Mechanical Engineering, University of Bristol, Bristol, U.K. Since 2010, he has been with the Faculty of Mechanical and Electrical Engineering, Kunming University of Science and Technology, Kunming, China, where he became a Professor in 2013. His current research interests include intelligent control, adaptive parameter estimation, neural network, and nonlinear control and application.

Dr. Na was a recipient of the Best Application Paper Award of the third IFAC International Conference on Intelligent Control and Automation Science (IFAC ICONS 2013) and the 2017 Hsue Shen Tsien Paper Award.